Performance Prediction for Fiber-Fed Microcellular Radio Network

R. S. Fyath* A. A. W. Al-Saffar** M. Sh. Abed*

* University of Basrah
College of Engineering
Department of Electrical Engineering

** Basrah Technical Institute
Computer Center

Abstract

The use of fiber-optic links as the connecting media in wireless microcellular networks can be provide uniform radio coverage to spatially distributed mobile users in cost effective manner. This paper investigates theoretically the performance of fiber distribution system for mobile phone networks that uses a single high power Nd:YAG laser in the base station and shared by many microcells. Analytical expressions are derived for the bit-error-rate (BER) floor characteristics and optimum operating conditions. The results indicate clearly that the laser power can be reduced significantly when the modulation index is optimized.

تقييم الأداء لشبكات التلفون الخلوي المرتبطة بخطوط فايبر–ضوئية

د. رعد سامي فياض* د. علاء عبدالوهاب حسن** مهند شريف عبد

الخلاصة

إن استخدام خطوط الاتصالات الضوئية لربط محطات الإرسال والاستلام في أنظمة التلفون الخلوي يقدم مرونة عالية مع التقليل في الكلفة. تقدم هذه الورقة تحليلا نظريا لهذا النظام في حالة استخدام مصدر ليزري واحد في المحطة الرئيسية وتقوم المحطات الثانوية بخدمته باستخدام هذا المصدر. تم اشتقاق معادلات رياضية تحدد مميزات معدل الخطأ والقيم المثلى لعمل هذا النظام.

1. Introduction

Transmission of microwave signals over optical fiber has been the subject of intense research for the past three years, mainly due to large bandwidth and low loss of optical fiber [1]. In a typical fiber-optic radio link, the amplitude of an optical carrier from a laser source at the central station is intensity modulated by radio subcarrier signals. After transmission via optical fibers, the modulated optical signals are detected, amplified and radiated at the radio stations for serving the subcarriers or mobile users.

Recently, a lot of efforts have been devoted into the use of fiber-optic links as the connecting infrastructure in wireless microcellular networks [2,3]. Microcellular systems, composed of small cells of hundred meters diameter, are attractive for personal communication services [4]. The introduction of microcells reduces power consumption and size of the handset, and utilizes the limited radio frequencies efficiently and therefore, providing a large capacity [5,6]. When a microcellular network is implemented using fiber-fed distributed antenna, the received radio frequency (RF) signals at each antenna are transmitted over a fiber-optic link to a central base station where all the

demultiplexing and signal processing are done.

There are some architectures proposed in the literature for microcellular systems incorporating fiber-optic links between the base station (BS) and the radio ports (RPs) [3,7]. However, these systems require a laser and its associated circuit to control the laser parameters such as temperature, output power, linearity ... etc. at each RP. Recently, Wu et al. [8] have proposed in a brief letter a new fiber distribution architecture for microcellular radio network where a single high power 1.3 μm Nd:YAG laser is employed at BS and shared by different groups of downstream signals. The system configuration with frequency reuse is shown in Fig. 1 [8]. The macrocell is divided into N_R x N_2 midcells and each midcell is divided into N_1 microcells. Here, N_R denotes the number of frequency reuse regions. For each region there are N_1 different groups of M-subcarrier radio signals. At RP, an optical coupler is used to split the optical power into two ways: one for the photodetector of the downstream and the other for the modulator of the upstream signals from the antenna (see Fig. 2). The structure simplifies the hardware complexity of RP while the total number of microcelles in the coverage of the BS is N_R x N_1 x N_2 .

The aim of this paper is to investigate in details the performance of the fiber distribution architecture proposed in [8]. Analytical expressions are derived to assess the optimum values of modulation index required to maximize the carrier-to-noise (CNR) at specific values of number of subcarrier signals.

2. System Analysis

For the downstream, the detected photocurrent at the RP is given by

$$i_R(t) = R\,C_c\,P_r\,[1+\cos\theta_B(t)] + n(t) \qquad (1)$$

where
R = Photodetector responsitivity.
C_c = Coupling ratio of the optical coupler.
P_r = Input optical power at the coupler.
θ_B = M-subcarrier radio signal from the BS.
n(t) = Additive noise.

The output power of the Nd:YAG laser is given by

$$P_s = \frac{N_R\,N_1\,N_2\,P_r}{L_e\,L_p} \qquad (2)$$

where
L_e = Insertion loss of the external amplitude modulator.
L_p = Propegation loss of the fiber.

The M-subcarrier radio signal is a composite microwave FSK signal generated by modulating individual voltage controlled oscillators (see Fig. 3) with baseband data stream. The modulated microwave subcarriers are summed, amplified, and then fed to the amplitude modulator to modulate the optical carrier. The composite microwave signal can be expressed by

$$\theta_B(t) = \sum_{k=1}^{M} \beta_k \cos[2\pi f_k t + \alpha_k(t)] \qquad (3)$$

where
β_k = Modulation index.
f_k = Microwave subcarrier frequency.

The FSK information for each data channel is contained in the term $\alpha_k(t)$.

Using equ. 3 into equ. 1, the photocurrent can be described using Bessel function expansion

$$i_R(t) = R\,C_c\,P_r \sum_{n_1=-\infty}^{\infty} \cdots \sum_{n_M=-\infty}^{\infty} \cdots J_{n_1}(\beta) \cdots J_{n_M}(\beta) \cos[n_1(f_1 t+\alpha_1(t)) + \cdots + n_M(f_M t+\alpha_M(t))] + n(t) \qquad (4)$$

where $J_n(\beta)$ is the nth order Bessel function of the first kind. In writing equ. 4, we have neglected the first term in equ. 1

since it is a dc term and hence contains no information. Further, we have assumed that β is identical for all the channels.

The FSK information for a particular channel is contained in the first order term of the Bessel series [9]. For example, the signal for the qth channel is found by setting $n_m = -1$ and the remaining indexes to zero [9]. The result is

$$i_{R_q}(t) = I_R \cos\left[2\pi f_q t + a_q(t)\right] \tag{5a}$$

$$I_R = R C_a P_r J_1(\beta) \left[J_0(\beta)\right]^{M-1} \tag{5b}$$

Note that $i_{R_q}(t)$ has the form of an FSK signal with a center frequency of f_q. The carrier-to-noise ratio (CNR), X_R, can be expressed as

$$X_R = \frac{0.5\, i_R^2}{N_{sh} + N_{th} + N_{RIN} + N_{3rd}} \tag{6}$$

where

N_{sh} = Shot noise.
N_{th} = Receive thermal noise.
N_{RIN} = Noise introduced by the relative intensity noise of the laser source.
N_{3rd} = 3rd order intermodulation distortion.

Equation 6 is written under the assumptions of

(i) Negligible 2nd-order intermodulation distortion. This assumption is justified when the transmission band is limited to a single octave [10].
(ii) Negligible adjacent channel crosstalk. This assumption is justified when spacing is greater than the bit rate is chosen.

The shot, thermal and intensity noise sources can be described by [11].

$$N_{sh} = 2\, e\, R\, C_a\, P_r\, B \tag{7a}$$

$$N_{th} = \frac{4 N_F K T B}{R_L} \tag{7b}$$

$$N_{RIN} = RIN \left(R C_a P_r\right)^2 B \tag{7c}$$

In equs. 7a-7c,
e = Electronic charge.
B = Signal bandwidth.
N_F = Amplifier noise figure.
K = Boltzmann's constant.
T = Absolute temperature.
R_L = Load resistance.
RIN = Relative intensity noise of the laser.

An expression describing the 3rd order intermodulation distortion is deduced from the analysis reported in [10]. For the system under observation, N_{3rd} is described by

$$N_{3rd} = \frac{h_3 k_3}{2}\left[R C_a P_r \left[J_1(\beta)\right]^2 \left[J_0(\beta)\right]^{M-3}\right]^2 \tag{8}$$

Where h_3 is the effective factor of 3rd-order intermodulation power within the desired signal band and equals to 0.66 for FSK modulated radio signal [10]. The parameter k_3 denotes the number of 3rd-order intermodulation products (IMPs) falls directly within the frequency band of the channel under consideration. The largest number of k_3, which falls on the central channel, is [8]

$$k_3 = \frac{M\left[\frac{M}{2}+1\right] + \left[(M-3)^2 - 5\right]}{4} \tag{9}$$

Where M is assumed to be even. Equation 9 can be solved to determine the number of channel M for a specific value of k_3. The result is

$$M = \frac{\left(10 + \sqrt{k_3 + 4}\right)}{6} \tag{10}$$

For $k_3 = 0$, $M = 2$ as expected.

The dependance of CNR on optical power P_r can be deduced by subsituting equs. 7 and 8 into equ. 6. The result is

$$X_R = \frac{A_2 P_R^2}{B_0 + B_1 P_R + B_2 P_R^2} \qquad (11)$$

Where

$$A_2 = \frac{1}{2}\left[R C_a J_1(\beta).[J_0(\beta)]^{M-1}\right]^2 \qquad (12a)$$

$$B_0 = \frac{4 N_F K T}{R_L} \qquad (12b)$$

$$B_1 = 2 e R C_a B \qquad (12c)$$

$$B_2 = RIN.R^2 C_a B + \frac{1}{2} h_3 k_3 \left[R C_a (J_1(\beta))^3.(J_0(\beta))^{M-3}\right]^2 \qquad (12d)$$

Equation 11 can be solved to determine the required optical power P_r to achieve a specific CNR

$$P_r = \frac{B_1 X_R + \sqrt{(B_1 X_R)^2 + 4 B_0 X_R (A_2 - B_2 X_R)}}{2(A_2 - B_2 X_R)} \qquad (13)$$

Equation 13 is one of the main result of this paper. An important observation to make is that, for a fixed 3rd-order intermodulation distortion, X_R converges to a finite value when $P_r \to \infty$. In other words, even if the signal power is infinity large, the bit-error-rate (BER) is finite. This phenomenon corresponds to so-called BER floor.

$$X_f = \mathrm{Lim}_{P_r \to \infty} X_R = \frac{A_2}{B_2} \qquad (14)$$

The BER of FSK system is given by [11]

$$P_e = \frac{1}{2}\,\mathrm{erfc}\sqrt{\frac{X_R}{2}}\,P_e \qquad (15)$$

where erfc(.) denotes error function complement.

When RIN is negligible, equ. 14 is simplified to

$$X_f = \left(\frac{1}{h_3 k_3}\right)\left[\frac{J_0(\beta)}{J_1(\beta)}\right]^4 \qquad (16)$$

In most practical cases, β is small and $J_0(\beta)$ and $J_1(\beta)$ can be approximated by 1 and $\beta/2$, respectively. Then equ. 16 is approximated to

$$X_f = \frac{16}{h_3 k_3 \beta^4} \qquad (17)$$

Equation 17 reveals that the BER floor decreases with increasing the modulation index β and the number of channels M.

3. Optimum Operating Conditions

Careful investigation of equs. 6-8 reveals that there is an optimum value for the modulation index β, β_{opt}, that maximizes the CNR at a specific value of P_r. The value of β_{opt} can be found by setting the derivative of equ. 6 with respect to β to zero. The result is

$$\beta_{opt} = 2\left[\frac{N_{th} + N_{sh}}{h_3 k_3 R^2 C_a^2 P_r^2}\right]^{\frac{1}{6}} \qquad (18)$$

where the RIN is assumed to be negligible and the Bessel functions are approximated to first order $J_0(\beta) = 1$ and $J_1(\beta) = \beta/2$.

At $\beta = \beta_{opt}$, $N_{th} + N_{sh} = 2N_{3rd}$ and hence equ. 18 can be rewritten as

$$\beta_{opt} = \frac{2}{(3 h_3 k_3 X_R)^{\frac{1}{4}}} \qquad (19)$$

The maximum value of CNR achieved at $\beta = \beta_{opt}$ is given by

$$(X_R)_{max} = \frac{16}{3 h_3 k_3 \beta_{opt}^2} \qquad (20)$$

Equation 19 indicates clearly that β_{opt} is inversely proportional to the fourth power of CNR and decreases with increasing the number of channel.

It is worth to mention here that the modulation index can be optimized to yield a minimum level of P_r at a specific value of CNR. The expressions for β_{opt} in this case are also described by equs. 18 and 19. The optimum value of P_r is given by

$$(P_r)_{min} = \frac{1}{R C_e \beta_{opt}} \sqrt{6 X_R (N_{th} + N_{sh})} \qquad (21a)$$

$$= \frac{1}{R C_e} \left[\frac{27}{4} h_3 k_3 X_R^2 \right]^{\frac{1}{4}} [N_{th} N_{sh}]^{\frac{1}{2}} \qquad (21b)$$

4. Simulation Results

Figure 4 illustrates the dependence of the largest number of the 3rd-order IMPs (k_3), which falls on the central channel, on the number of channels (M). Note that k_3 increases dramatically with M. At M=50 (100), k_3 approaches 876 (3626). This indicates that k_3 is approximately proportional to M^2 and this result can be predicted from equ. 9 under the assumption of large values of M.

To assess the performance of the downstream channels, the following parameter value are used to simulate the following results:

Amplifier noise figure, N_F = 4 dB.
Amplifier load resistance, R_L =50 ohm.
Signal bandwidth, β = 100 KHz.
Relative intensity noise of the laser Source, RIN = -165 dB/Hz.
Photodetector responsitivity, R = 1.
Coupling ratio of the optical coupler, C_e=0.5.

These values yield, a required input optical power at the coupler (P_r) of –22.96, -28.32, and –30.6 dBm for β = 0.1, 0.2, and 0.3, respectively, and assuming CNR = 20 dB and M=1 (i.e., absence of 3 rd-order intermodulation distortion). Note that the receiver sensitivity is enhanced (i.e., P_r reduces) with increasing β when the intermodulation distortion is negligible.

The dependence of P_r on M is depicted in Fig. 5 for CNR =20 dB and different values of β. The results indicate clearly that P_r increases rapidly with M and this effect is more pronounced at large β. At a given value of M, P_r tends to ∞ which indicates the occurrence of BER floor. This characteristic is illustrated further in Figs.6 and 7. In Fig.6, we plot the upper limit of CNR, X_f, that can be used without the occurrence of BER floor as a function of M. Figure 7 illustrates the dependence of BER floor on M for β = 0.1, 0.2 and 0.3. Investigating Figs. 6 and 7 reveals that the upper value of M should be limited to 135, 35, and 16 for β = 0.1, 0.2, and 0.3, respectively to reduce the BER floor below 10^{-9} (i.e., X_f = 15.5 dB).

Figure 8 shows the dependence of the power P_r on the modulation index β and number of channels M for a CNR = 20 dB. Investigating this figure highlights the following fact: There is an optimum value for β that minimizes P_r and this value is more critical when M is large. The variations of optimum value of the modulation index β_{opt} and the corresponding minimum value of optical power $(P_r)_{min}$ with M are plotted in Figs. 9a and 9b, respectively, and for two values of CNR, 15 dB and 20 dB. Note that β_{opt} decreases with M while $(P_r)_{min}$ increases with M. Note further that the effect of CNR on β_{opt} and $(P_r)_{min}$ is almost independent of M. Table-1 summarizes the main results drawn from Fig. 9. Note that for M = 50 and CNR = 20 dB, the optimum value of P_r

is –21.4 dBm. This value is to be compared with P_r = -25.1 dBm in the absence of 3rd-order intermodulation distortion. Thus even at optimum conditions, the power penalty due to the 3 rd-order IMPs is as high as 3.7 dB for this case.

5. Discussion and Conclusions

To take an idea about the optical power of the Nd:YAG laser required to support this system, we consider the following parameters

$N_1 = N_2 = 4$ $N_R = 25$ $M = 50$

Insertion loss of the external amplitude modulator = 10 log $(1/L_e)$= 3 dB.

Propagation fiber loss=10 log$(1/L_p)$=4 dB. (i.e., 1o Km of fiber with loss 0.4 dB).

When β is optimized, then P_r = -21.4 dBm is needed to achieve a CNR - 20 dB. If 5 dB power margin is allowed for each optical link, then the output laser power P_s = 46 mW (from equ.2). Such level of P_s can be obtained easily with current Nd:YAG laser [11]. The total channels supported by above example is equal to 20000 (4x 4x 25 x 50) channels.

In summary, this paper has investigated theoretically the performance of a fiber distribution system for microcellular radio network. The main feature of this system is that it incorporates a single laser source at the base station and shared by many microcells. The results indicate that the modulation index must be optimized to reduce the power requirement of the laser source. The expressions and simulation results developed here can be used as a guideline to design this system under optimum conditions and to assess the influence of intermodulation distortion on system performance.

References

[1] Q. Z. Liu, R. Davis, and R. I. MacDonald," Fiber-optic microwave link with monolithic integrated optoelectronic," IEEE Photon Technol. Lett., vol. 7, no. 5, pp. 567-569, 1995.

[2] W. I. Way," Optical fiber-based microcellular systems: An overview," IEICE Trans. Commun.,vol. E76-B, no. 9, pp. 1091-1102, 1993.

[3] M. Shibutani, T. Kanai, W. Domom, K. Emura, and J. Namiki," Optical fiber feeder for microcellular mobil communication systems," IEEE J. Select. Areas. Commun.,vol. 11, no. 7, pp. 1118-1126,1993.

[4] H. Kim, J.M. Cheong, C. –H. Lee, and Y. C. Chung," Passive optical network for microcellular CDMA personal communication services," IEEE Photon Technol. Lett., vol. 10, no. 11, pp. 1641-1643, 1998.

[5] D. M Cutrer, J.B. George, T. H. Le, and K. Y. Lau," Dynamic range requirements for optical transmitters in fiber-fed microcellular networks," IEEE Photon. Technol. Lett., vol. 7, no. 5, pp. 564-566, 1995.

[6] L. J. Greenstein, N. Amitay, and T. S. Chu," Microcells in personal communication systems," IEEE Commun. Mag., vol. 30, pp. 76-89, 1992.

[7] T. S. Chu and M. J. Gans," Fiber-optic microcellular radio," IEEE Trans. Vechicular Tech., vol. 8, pp. 599-607, 1991.

[8] J. Wu, J. –S. Wu, and H. –W. Tsao," A fiber distribution system for microcellular radio," IEEE Photon. Technol. Lett., vol. 6, no. 9, pp. 1150-1152, 1994.

[9] R. Cross and R. Olshansky," Multicannel coherent FSK experiments using subcarrier multiplexing technique," J. of Lightwave Technology, vol. 8, no. 3, pp. 406-415, 1990.

[10] R. Cross and R. Olshansky," Third order intermodulation distortion in coherent subcarrier multiplexed system," IEEE Photon Technol., vol. PTL-1, pp. 91-93, 1989.

[11] M. M. Liu," Principles and applications of optical communications," McGraw-Hill Co., USA, 1996.

Number of channels	CNR=20 dB		CNR=20 dB	
	β_{opt}	$(P_r)_{min}$	β_{opt}	$(P_r)_{min}$
10	0.236	-25.115	0.315	-28.389
20	0.156	-23.458	0.212	-26.779
50	0.098	-21.381	0.131	-24.726

Table-1: Optimum parameter as a function of M and CNR

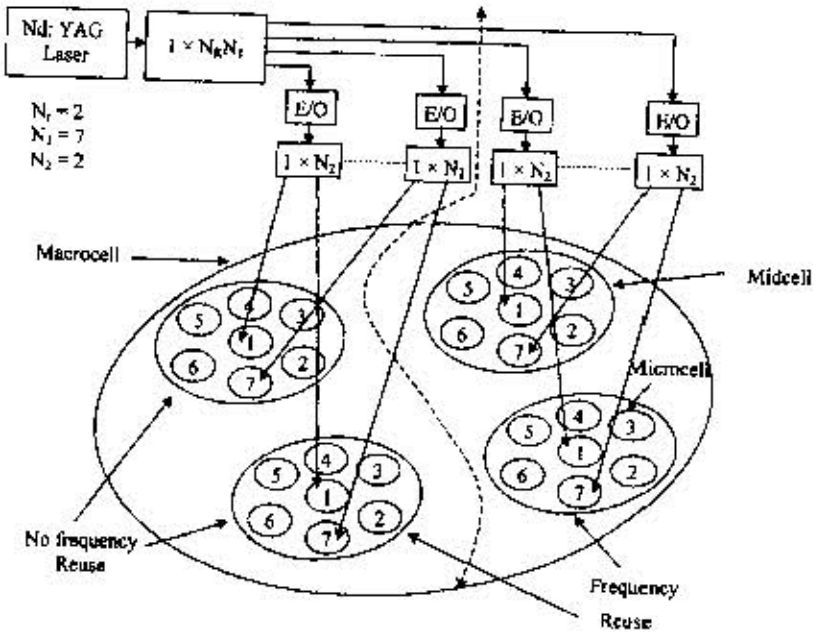

Fig.1: Conceptual diagram for the radio over fiber distribution system with the frequency reuse scheme (after [7]), where E/O = electrical to optical converter

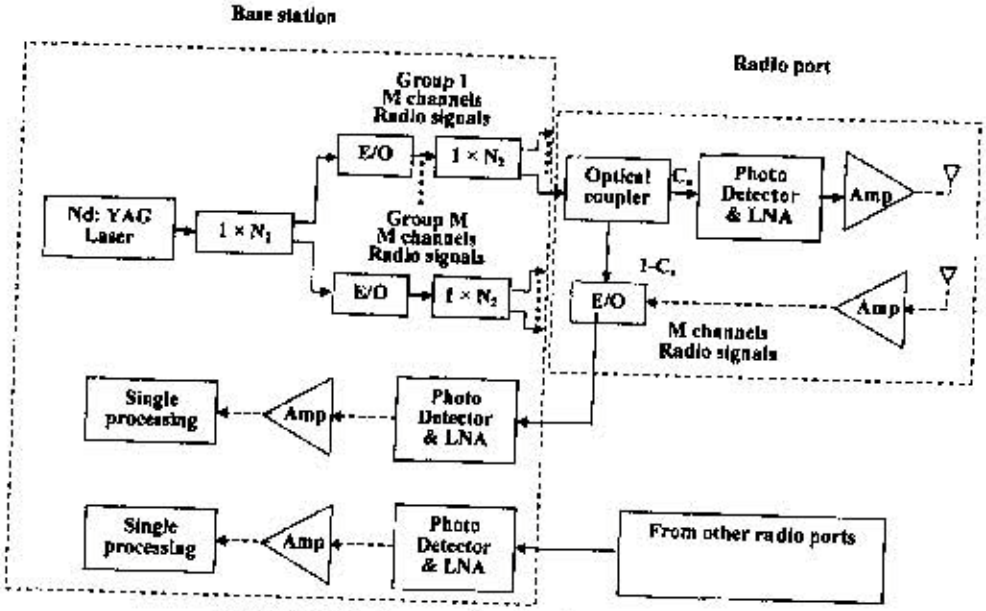

Fig 2: Block diagram for the fiber-radio link
where LNA: low noise amplifier,
——— : Optical signal
- - - - - - - : Electrical signal

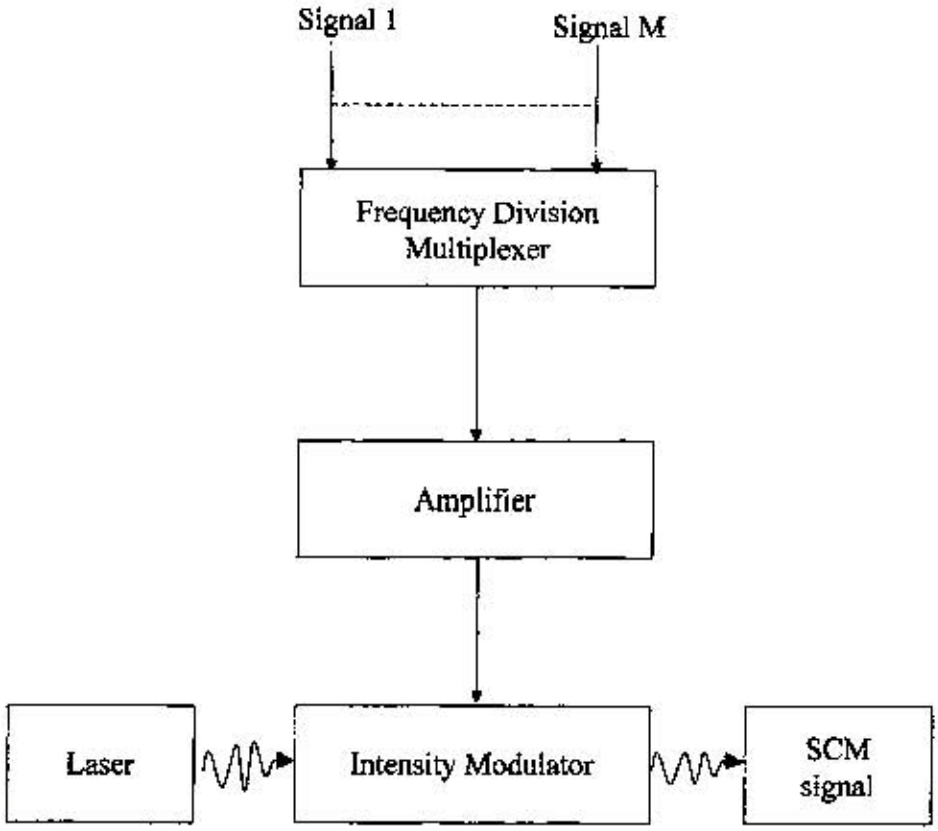

Fig. 3: Schematic diagram of a subcarrier multiplexed (SCM) system.

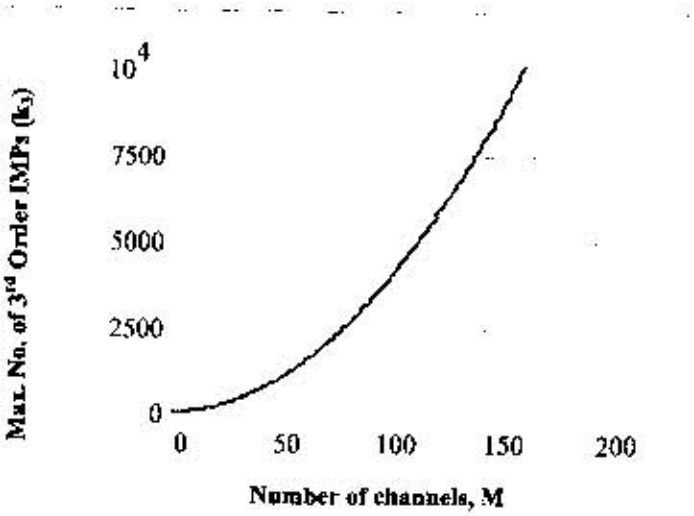

Fig.4: Maximum number of 3rd-order IMPs (falling in the central channel) as a function of number of channels.

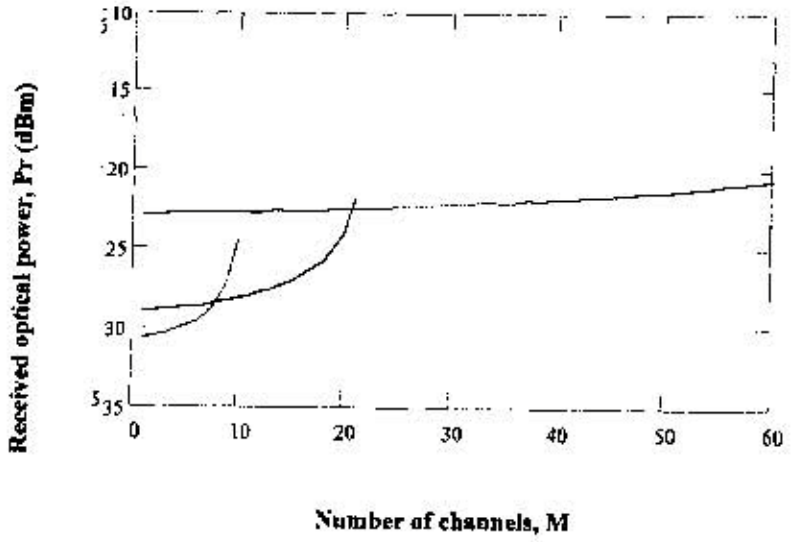

Fig. 5: Dependence of received optical power on number of channels assuming CNR = 20 dB.

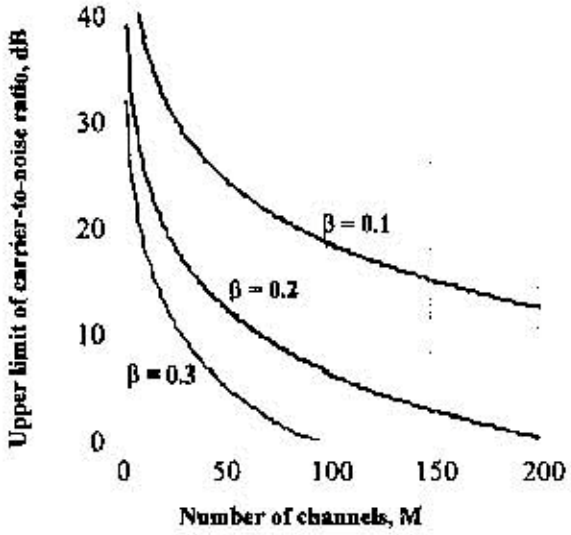

Fig. 6: Upper limit of carrier to noise ratio (CNR) as a function of number o channels for different values of modulation index.

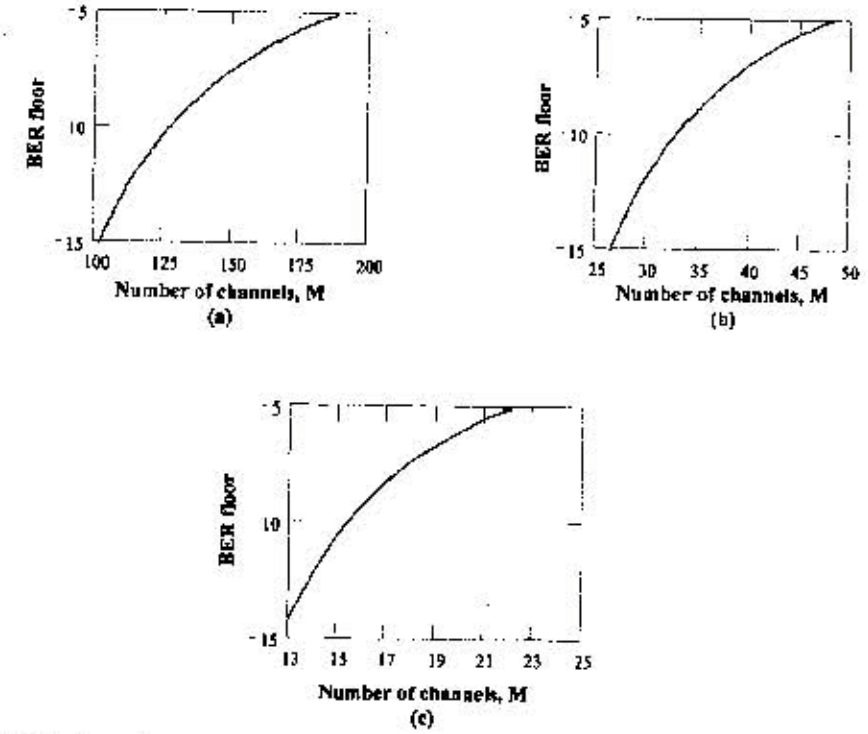

Fig. 7: Dependence of BER floor characteristics on number of channels.
(a) Modulation index = 0.1 .
(b) Modulation index = 0.2 .
(c) Modulation index = 0.3 .

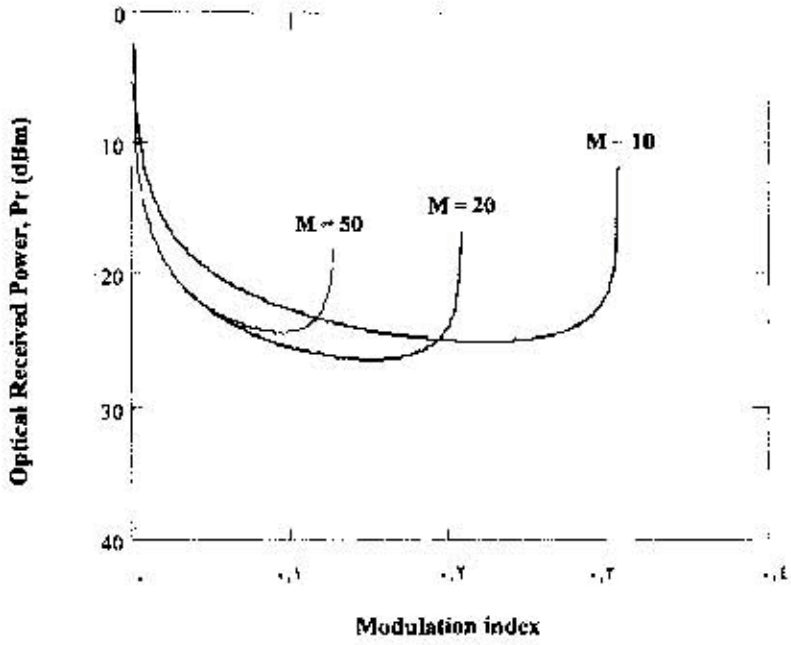

Fig. 8: Effect of modulation index on received optical power required to achieve a CNR = 20 dB.